

Preparation, XRD and Raman spectroscopic studies on new compounds $RE_2Hf_2O_7$ ($RE = Dy, Ho, Er, Tm, Lu, Y$): Pyrochlores or defect-fluorite?

B.P. Mandal, Nandini Garg¹, Surinder M. Sharma¹, A.K. Tyagi*

Chemistry Division, Bhabha Atomic Research Centre, Mumbai 400 085, India

Received 3 January 2006; received in revised form 23 March 2006; accepted 26 March 2006

Available online 1 April 2006

Abstract

A series of compositions with the general formula $RE_2Hf_2O_7$ ($RE = Dy, Ho, Er, Tm, Y$ and Lu) was prepared by a standard solid-state route and characterized by powder X-ray diffraction (XRD) and Raman spectroscopy. As per theoretical modeling reported in literature, some of these materials were predicted to exist in pyrochlore lattice. However, a careful X-ray diffraction, Raman spectroscopic and synchrotron radiation-XRD study revealed that under the experimental conditions used in the present investigation, out of all the $RE_2Hf_2O_7$ samples only $Dy_2Hf_2O_7$ has got a tendency to form a pyrochlore structure. All the other (Ho, Er, Tm, Lu, Y) hafnates crystallize in a defect-fluorite structure. In order to further ascertain these inferences, a few more $RE_2Hf_2O_7$ samples (La, Nd, Sm) i.e., with larger RE^{3+} ions were also prepared and the results were compared.

© 2006 Elsevier Inc. All rights reserved.

Keywords: Ceramics; X-ray diffraction (XRD); Raman spectroscopy

1. Introduction

The pyrochlores have the general formula $A_2B_2O_7$ where A is the larger cation and B is the smaller one. Mostly A is a trivalent rare-earth ion, but can also be a mono, divalent cation, and B may be $3d, 4d$ or $5d$ transition element having an appropriate oxidation state required for charge balance to give rise to the composition $A_2B_2O_7$. The space group of the ideal pyrochlore is $Fd\bar{3}m$ [1]. The pyrochlore structure is reported [2,3] as a network consisting of corner linked BO_6 octahedra with A atoms filling the interstices. Some pyrochlores exist as insulators whereas some others are semiconductors [4]. There are a few pyrochlores exhibiting dielectric, piezoelectric and ferroelectric properties, if A and B remain in highest oxidation state [1]. Immobilization of plutonium, americium and other minor actinides and the long-lived fission

products is another futuristic potential application of pyrochlores [5]. In view of these wide ranging applications, the pyrochlores have attracted the attention of theoreticians also who are predicting the existence of new pyrochlores. Recently, Rushton et al. [6] used the CASCADE and GULP codes to predict the pyrochlore-to-fluorite disorder temperature for several $A_2Zr_2O_7$ compounds ($A = Nd, Sm, Eu, Gd, Dy, Y$, etc.). Similarly Stanek and Grimes [7] had predicted the existence of a few hafnium-based pyrochlores based on theoretical calculations. According to these studies the predicted transformation temperatures for $Dy_2Hf_2O_7$, $Ho_2Hf_2O_7$ and $Er_2Hf_2O_7$ were found to be close enough to the experimental value for $Gd_2Zr_2O_7$, suggesting that these hafnates also can be crystallized with the pyrochlore structure as observed for $Gd_2Zr_2O_7$. Since research on pyrochlores is an ongoing activity in our group it was felt that preparation of these hafnates would be worthwhile as they could be potential materials from the point of view of host lattices for minor actinide transmutation using an accelerator driven sub-critical system.

*Corresponding author. Fax: +91 22 2550 5151.

E-mail address: aktyagi@barc.ernet.in (A.K. Tyagi).

¹Synchrotron Radiation Section.

2. Experimental

AR grade RE_2O_3 ($RE = La, Nd, Sm, Dy, Ho, Er, Tm, Lu, Y$) and HfO_2 were first heated at $900^\circ C$ overnight to remove moisture and other volatile impurities, if any. Stoichiometric amounts of the reactants were weighed to get the compositions corresponding to $RE_2Hf_2O_7$. The homogenized mixtures were then subjected to a three-step heating protocol as follows with intermittent grindings. The thoroughly ground mixtures were heated in the pellet form at $1200^\circ C$ for 36 h, followed by a second heating at $1300^\circ C$ for 36 h after regrinding and repelletizing. In order to attain a better homogeneity, the products obtained after second heating were again reground, pelletized and heated at $1400^\circ C$ for 48 h. All the products were analyzed by powder X-ray diffraction (XRD). Subsequently one more heat treatment at $1700^\circ C$ for 6 h was given to each sample to investigate the existence of pyrochlore structure after this heat treatment. The heating and cooling rates were 2° per minute in all the annealing steps and atmosphere was static air. The XRD patterns of all the $RE_2Hf_2O_7$ products were recorded on Philips X'pert Pro XRD unit with monochromatized $CuK\alpha$ radiation ($K\alpha_1 = 1.5406 \text{ \AA}$ and $K\alpha_2 = 1.5444 \text{ \AA}$) operated at 1.2 kW power. The patterns were analyzed using POWDERX program. The silicon was used as an external standard for calibration of the instrument.

Unpolarized Raman scattering data, on each sample in pellet form, were collected in the 45° geometry (i.e., the collection of Raman spectra is at an angle of 45° to the incident laser beam) with the help of a CCD-based single stage spectrograph. The 532 nm line of a solid-state diode laser was used as an excitation source. An appropriate super-notch filter was used to cut off the Rayleigh scattered light of the laser. The X-ray diffraction data on polycrystalline powder of $Dy_2Hf_2O_7$ in a $100 \mu m$ glass capillary was collected at the Elletra synchrotron source ($\lambda = 0.6972 \text{ \AA}$). The diffraction rings were recorded on a Mar imaging plate system, and in order to take care that there is no effect of texture the capillary was given a small oscillation during data collection. The two-dimensional images were converted to one-dimensional diffraction patterns using the FIT2D software [8].

3. Results and discussion

A careful analysis of the XRD patterns recorded using the laboratory XRD unit revealed that none of the products was found to have pyrochlore type lattice, as the typical super-lattice peaks at $2\theta \approx 14^\circ, 27^\circ, 36^\circ, 50^\circ$, etc. (using $CuK\alpha$ X-ray source) for (111), (311), (331), (531), respectively, corresponding to pyrochlore lattice were absent. The limiting radius ratio (r_A/r_B) for the stabilization of the pyrochlore lattice, $A_2B_2O_7$, is reported [9] to be from 1.2 to about 1.6 at 1 atm. The upper limit of the radius ratio can be further increased by applying high pressure. Thus based on the radius ratio (Table 1), one

Table 1

Lattice parameters (\AA) for different compositions in $RE_2Hf_2O_7$ ($RE = Dy, Ho, Er, Tm, Lu$ and Y), along with the radius ratio (r_A/r_B)

Composition	Lattice parameter(\AA)	Radius ratio (r_A/r_B)
$Dy_2Hf_2O_7$	5.201 (1)	1.332
$Ho_2Hf_2O_7$	5.200 (1)	1.315
$Er_2Hf_2O_7$	5.179 (1)	1.300
$Tm_2Hf_2O_7$	5.167 (1)	1.285
$Lu_2Hf_2O_7$	5.148 (1)	1.256
$Y_2Hf_2O_7$	5.196 (1)	1.314

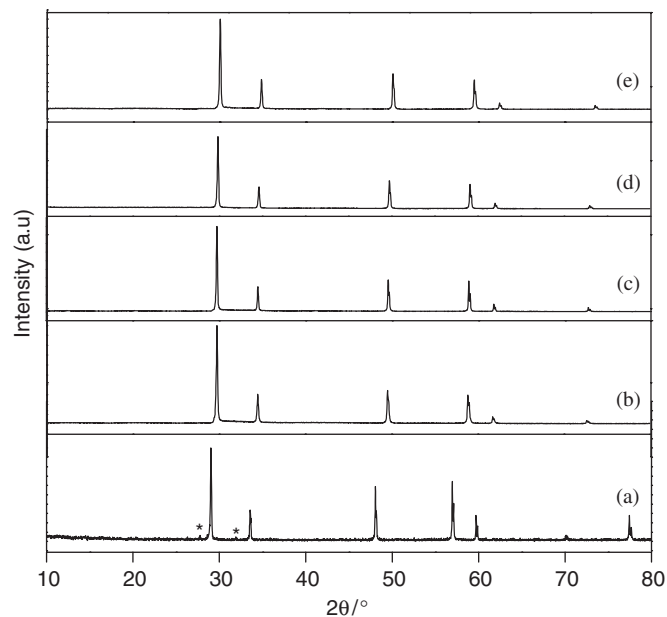


Fig. 1. Few XRD patterns of: (a) $La_2Hf_2O_7$, (b) $Dy_2Hf_2O_7$, (c) $Ho_2Hf_2O_7$, (d) $Er_2Hf_2O_7$, and (e) $Lu_2Hf_2O_7$ after heating at $1700^\circ C$.

would expect that at least $Dy_2Hf_2O_7$ might adopt a pyrochlore lattice (the ionic radius of various ions was taken from Ref. [10]). In order to rule out the absence of pyrochlore phase for these materials due to any kinetic barrier, these products were again ground and heated at $1700^\circ C$ for 6 h, followed by slow cooling to room temperature. The characteristic pyrochlore peaks were absent in the XRD pattern even after this heat treatment. Thus, it can be inferred that the absence of pyrochlore phase in this system is not due to any kinetic barrier. Typical XRD pattern of some $RE_2Hf_2O_7$ are shown in Fig. 1. The cell parameters, in conformity with the fluorite phase, for the products were calculated using least-squares methods and are given in Table 1. The variation of cell parameters as a function of RE^{3+} follows a trend as expected from the lanthanide contraction. The absence of pyrochlore phase in this series, as seen by laboratory PXRD data, can be attributed to the low radius ratio (Table 1). It is reported in literature [9] that if the radius ratio is close to 1.2, $A_2B_2O_7$ pyrochlore becomes $A_{0.5}B_{0.5}O_{1.75}$ defect-fluorite via random distribution of A

and *B* cations. Therefore, it is not surprising that the Dy and other smaller rare-earth hafnates prepared in the present investigation appear to adopt a defect-fluorite lattice, based on XRD data. As the radius ratio is increased from 1.2, one gets clear pyrochlore superstructure peaks. It may be noted that some deviations from this range of stability of pyrochlore (1.2–1.6) are also observed and this limiting radius ratio should be used only as a broad guideline. For instance, $\text{Er}_2\text{Ti}_2\text{O}_7$ ($r_A/r_B = 1.66$) forms a highly ordered pyrochlore whereas $\text{Er}_2\text{Zr}_2\text{O}_7$ ($r_A/r_B = 1.39$) forms a defective-pyrochlore lattice [11].

However, it may be added that the Raman spectroscopic investigation provides an unequivocal information [12] to distinguish between a defect-fluorite material and the so-called pyrochlore with the radius ratio close to the pyrochlore and defect-fluorite border. Therefore, these hafnates were investigated by Raman spectroscopy also. The Raman spectra of a pyrochlore structure has six Raman active modes according to group theory, which are $\Gamma = A_{1g} + E_g + 4F_{2g}$ and the fluorite structure has only one Raman active mode $\Gamma = F_{2g}$. The Raman spectra of the fluorites has a single broad band as the seven oxygen ions in the fluorite structure are randomly distributed over the eight anion sites which gives rise to disorder. Due to this disorder the Raman spectrum is reduced to a broad

continuum of density of states. Raman spectra of all the $\text{RE}_2\text{Hf}_2\text{O}_7$ ($\text{RE} = \text{La, Nd, Sm, Dy, Ho, Er, Tm, Lu, Y}$) compounds in this series are shown in Fig. 2. The Raman spectra recorded on powder of $\text{Dy}_2\text{Hf}_2\text{O}_7$ is also included in Fig. 2. The distinct Raman bands can be seen from the compacted sample (Fig. 2e) of $\text{Dy}_2\text{Hf}_2\text{O}_7$ whereas the Raman spectra from just the powder show a very broad band. It could be due to better signal-to-noise ratio from the compacted disks. The broadening cannot be attributed to small particle size as the diffraction pattern which was collected on powder samples of DyHf_2O_7 does not show any line broadening due to small particle size. The Raman modes were observed at 200, 326, 400, 612 and 872 cm^{-1} . A few weak Raman bands were also observed at 528, 693, 746 cm^{-1} . On comparing it with the spectra of lanthanum hafnate (Fig. 2a) having a pyrochlore structure we can assign the Raman modes of $\text{Dy}_2\text{Hf}_2\text{O}_7$ at 326 cm^{-1} to F_{2g} , 400 cm^{-1} to E_g and 612 cm^{-1} to F_{2g} [14]. The extra Raman modes at 200 and 872 cm^{-1} could be due to the distortion of the octahedra [14]. The broad band at 528 cm^{-1} can be attributed to the A_{1g}/F_{2g} Raman mode and the broad bands at 693 and 746 cm^{-1} can be attributed to the seven coordinated *A* cations as observed in the disordered fluorite phase by Glerup et al. [12]. However, the single band observed at $\sim 466 \text{cm}^{-1}$ in the fluorite structured

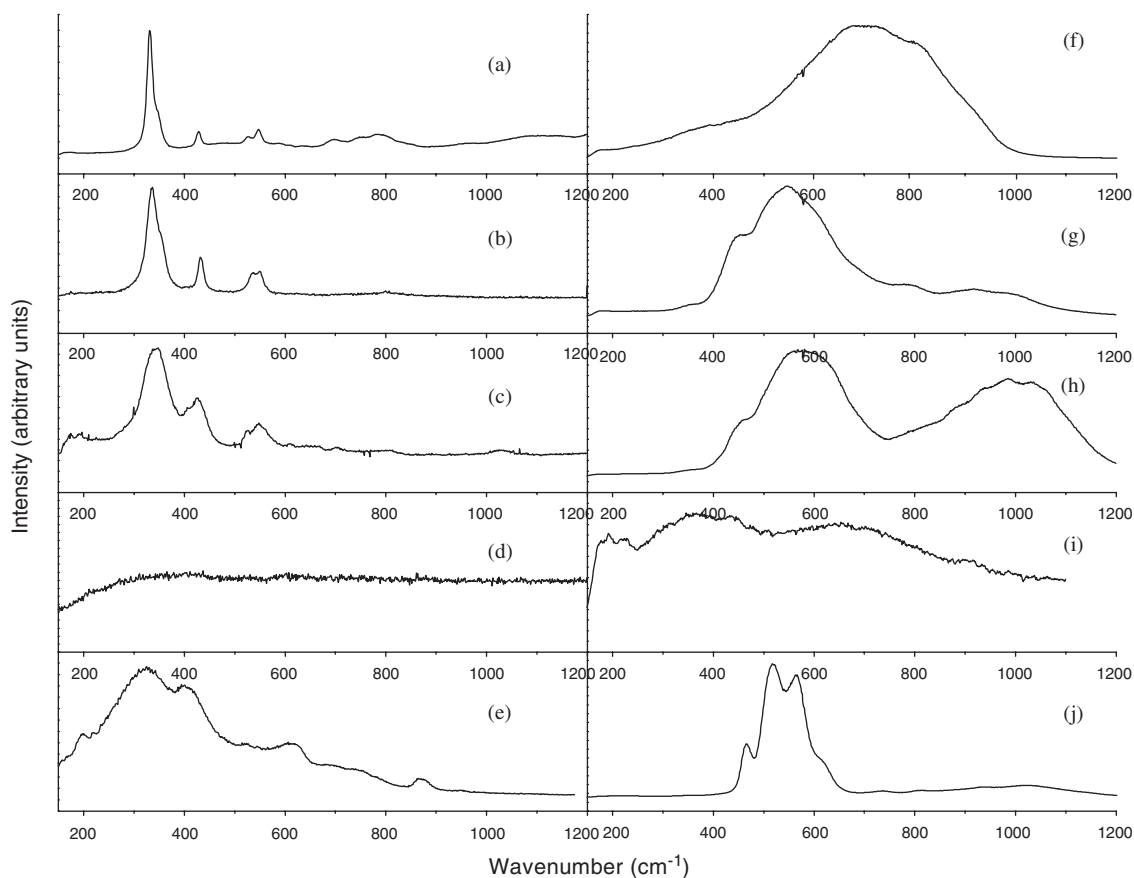


Fig. 2. Raman spectra of: (a) $\text{La}_2\text{Hf}_2\text{O}_7$, (b) $\text{Nd}_2\text{Hf}_2\text{O}_7$, (c) $\text{Sm}_2\text{Hf}_2\text{O}_7$, (d) $\text{Dy}_2\text{Hf}_2\text{O}_7$ (powder form), (e) $\text{Dy}_2\text{Hf}_2\text{O}_7$ (pellet form), (f) $\text{Ho}_2\text{Hf}_2\text{O}_7$, (g) $\text{Y}_2\text{Hf}_2\text{O}_7$, (h) $\text{Er}_2\text{Hf}_2\text{O}_7$, (i) $\text{Tm}_2\text{Hf}_2\text{O}_7$, and (j) $\text{Lu}_2\text{Hf}_2\text{O}_7$. The sharp peaks in the spectra of $\text{Lu}_2\text{Hf}_2\text{O}_7$ are probably due to some impurity present in the sample.

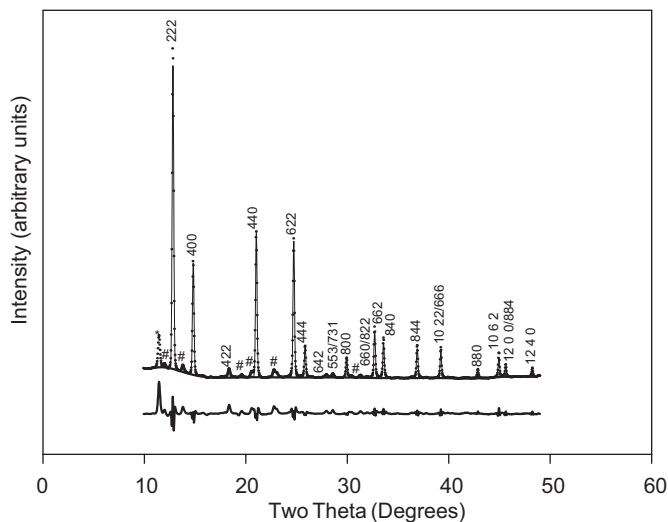


Fig. 3. Diffraction pattern of $\text{Dy}_2\text{Hf}_2\text{O}_7$. The (#) marks the diffraction lines from the unreacted HfO_2 and Dy_2O_3 . The diffraction line marked with the (*) could not be identified and maybe originating from some impurity.

oxides ThO_2 , CeO_2 , etc., was not observed by us [15]. Thus it can be seen clearly that even though the Raman spectra of $\text{Dy}_2\text{Hf}_2\text{O}_7$ can be compared with the other pyrochlore hafnates but it is not truly ordered also as it has broad Raman bands. It has been observed by Glerup et al. [12] that on introducing a cation disorder in $\text{Y}_2\text{Ti}_2\text{O}_7$ by doping it with Zr the A_{1g}/F_{2g} Raman mode observed at 531 cm^{-1} (corresponding mode in hafnate should have appeared at 528 cm^{-1}) loses intensity and becomes broad as the concentration of the dopant is increased [12]. Even Raman spectra of $\text{Dy}_2\text{Hf}_2\text{O}_7$ shows that the Raman mode at 528 cm^{-1} is hardly visible. These results clearly indicate that the $\text{Dy}_2\text{Hf}_2\text{O}_7$ sample synthesized by us does not attain a pure pyrochlore structure contrary to the predictions of Rushton et al. [6] but it has a tendency to form a pyrochlore lattice. It can be clearly seen that for $\text{RE}_2\text{Hf}_2\text{O}_7$ ($\text{RE} = \text{Y, Ho, Er, Tm, Lu}$) the Raman spectra is very broad even in the pellet form thereby indicating that these materials are defect-fluorite. The sharp bands observed for $\text{Lu}_2\text{Hf}_2\text{O}_7$ are due to luminescence possibly from some impurity atoms. However, the Raman spectra of $\text{RE}_2\text{Hf}_2\text{O}_7$ ($\text{RE} = \text{La, Nd, Sm}$) clearly indicate that these hafnates have crystallized in the pyrochlore structure as has also been reported in literature [13].

In order to further substantiate the fact that the $\text{Dy}_2\text{Hf}_2\text{O}_7$ could be a weakly ordered pyrochlore, it was studied by using synchrotron radiation source at Elletra, Italy as sometimes it is difficult to observe the very weak superstructure peaks using laboratory X-ray source. The X-ray diffraction pattern of $\text{Dy}_2\text{Hf}_2\text{O}_7$, recorded at Elletra, is shown in Fig. 3. A few weak peaks indeed appeared in the XRD pattern. The XRD pattern could be refined with the pyrochlore structure. The refined parameters are given in Table 2. The diffraction lines marked with * are due to

Table 2

Structural parameters for $\text{Dy}_2\text{Hf}_2\text{O}_7$ at ambient condition

Atom	Site	x	y	z
Dy	16d	0.5000	0.5000	0.5000
Hf	16c	0.0000	0.0000	0.0000
O	48f	0.348 (9)	0.125	0.125
O	48f	0.375	0.375	0.375

The space group is $Fd\bar{3}m$ and the lattice parameters are $a = 10.3900 \pm 0.0004 \text{ \AA}$.

the unreacted oxides of Dy and Hf, which could not be seen by a laboratory XRD data. One diffraction line at $2\theta = 11.45^\circ$ could not be indexed to any of the reactants or the product. It may be coming from some contaminant. It can be clearly seen that the (111) diffraction peak has no visible intensity. It has been shown by Dickson et al. that the intensity of the (111) reflection is the most sensitive to the position of the 48 (f) x -parameter of oxygen [16]. Its intensity diminishes as the x -parameter approaches that of the fluorite structure. On carrying out a Rietveld analysis (goodness of fit parameters $R_{\text{wp}} = 0.11$, $R(F^2) = 0.14$) of the diffraction pattern, with the pyrochlore structure the value of the cell constant and the x -parameter were determined to be $10.3900(4) \text{ \AA}$ and 0.348, respectively, which indicates that the structure could be close to pyrochlore as the x -parameter for the pyrochlore structure should lie between 0.3125 and 0.375 [1]. However, it is also observed that the reflections from planes having only oxygen atoms, i.e. (422) and (642) which are barely visible in a true pyrochlore have a visible intensity in $\text{Dy}_2\text{Hf}_2\text{O}_7$. This indicates that there is some rearrangement associated with the oxygen atoms. A literature search for Dy-based pyrochlores reveals the presence of only two fully ordered pyrochlores, i.e., $\text{Dy}_2\text{Ru}_2\text{O}_7$ and $\text{Dy}_2\text{Sn}_2\text{O}_7$ [17,18]. The radius ratio for $\text{Dy}_2\text{Ru}_2\text{O}_7$ and $\text{Dy}_2\text{Sn}_2\text{O}_7$ are 1.524 and 1.370, respectively, which are higher than that for $\text{Dy}_2\text{Hf}_2\text{O}_7$. Thus it can be inferred that a lower radius ratio in case of $\text{Dy}_2\text{Hf}_2\text{O}_7$ does not facilitate absolutely distinct positions for Dy^{3+} and Hf^{4+} ions, which is a prerequisite to the formation of a fully ordered pyrochlore structure. $\text{M}_2\text{Hf}_2\text{O}_7$ ($\text{M} = \text{La, Nd, Sm}$) crystallize in fully ordered pyrochlore phase which are obvious from Raman spectra, because their radius ratio 1.50, 1.43 and 1.39, respectively, are well within the limiting radius ratio of the pyrochlores. However, unlike $\text{RE}_2\text{Hf}_2\text{O}_7$ ($\text{RE} = \text{Ho, Er, Tm, Yb, Lu}$ and Y), which are unequivocally defect-fluorites, in case of $\text{Dy}_2\text{Hf}_2\text{O}_7$ there is competition between defect-fluorite and pyrochlore lattices.

4. Conclusions

The Raman results combined with the X-ray results indicate that the $\text{Dy}_2\text{Hf}_2\text{O}_7$ material prepared by us does not have a fully ordered pyrochlore structure but has a disordered pyrochlore structure. It has a tendency to attain

the pyrochlore structure and probably might become a true pyrochlore under some other thermodynamical conditions. A partially ordered $\text{Dy}_2\text{Hf}_2\text{O}_7$ might become fully ordered $\text{Dy}_2\text{Hf}_2\text{O}_7$, if synthesized at high pressure and high temperature (HP–HT). However, such a HP–HT synthesis needs to be performed to support this.

Acknowledgments

Dr. S.K. Kulshreshtha, Head, Chemistry Division is thanked for his keen interest in this work. Mr. H.K. Poswal, BARC, is thanked for helping with the Raman experiments and for useful discussions.

References

- [1] M.A. Subramanian, G. Aravamudan, G.V. Subba Rao, *Prog. Solid State Chem.* 15 (1983) 55.
- [2] F. Jona, G. Shirane, R. Pepinsky, *Phys. Rev.* 98 (1955) 903.
- [3] H. Nyman, S. Andersson, B.G. Hyde, M. O'Keeffe, *J. Solid State Chem.* 26 (1978) 123.
- [4] H.H. Kung, J.S. Jarrett, A.W. Sleight, A. Ferretti, *J. Appl. Phys.* 48 (1977) 2463.
- [5] H. Kleykamp, *J. Nucl. Mater.* 275 (1999) 1.
- [6] M.J.D. Rushton, R.W. Grimes, C.R. Stanek, S. Owens, *J. Mater. Res.* 19 (2004) 1603.
- [7] C.R. Stanek, R.W. Grimes, *J. Am. Ceram. Soc.* 85 (2002) 2139.
- [8] A.P. Hammersley, S.O. Svensson, M. Hanfland, A.N. Fitch, D. Hauserman, *High Pressure Res.* 14 (1996) 235.
- [9] D.J.M. Bevan, E. Summerville, in: K.A. Gschneider Jr., L. Eyring, (Eds.), *Handbook on the Physics and Chemistry of Rare-earths*, vol. 3, North-Holland, Amsterdam, 1979, p. 496.
- [10] R.D. Shanon, *Acta Crystallogr. A* 32 (1976) 751.
- [11] K.E. Sickafus, L. Minervini, R.W. Gromes, J.A. Valdez, M. Ishimaru, F. Li, K.J. McClellan, T. Hartmann, *Science* 289 (2000) 748.
- [12] M. Glerup, O.F. Nielsen, F.W. Poulsen, *J. Solid State Chem.* 160 (2001) 25.
- [13] N.V. Gundovin, F.M. Spiridonov, L.N. Komissarova, K.I. Petrov, *Russ. J. Inorg. Chem.* 20 (1975) 325.
- [14] M.T. Vandenborre, E. Husson, J.P. Chatry, D. Michel, *J. Raman Spectrosc.* 14 (1983) 63.
- [15] V.G. Keramidis, W.B. White, *J. Chem. Phys.* 59 (1973) 1561.
- [16] S.J. Dickson, K.D. Hawkins, T.J. White, *J. Solid State Chem.* 82 (1986) 146.
- [17] T. Yamamoto, R. Kanno, Y. Takeda, O. Yamamoto, M. Takano, *J. Solid State Chem.* 109 (1994) 372.
- [18] B.J. Kennedy, *Mater. Sci. Forum* 228 (1996) 753.